

# Bayesian analysis of the kinetics of quantal transmitter secretion at the neuromuscular junction

Anatoly Saveliev<sup>1</sup> · Venera Khuzakhmetova<sup>1,2</sup> · Dmitry Samigullin<sup>1,2,3</sup> ·  
Andrey Skorinkin<sup>1,2</sup> · Irina Kovyazina<sup>1,2</sup> · Eugeny Nikolsky<sup>1,2,4</sup> · Ellya Bukharaeva<sup>1,2</sup>

Received: 20 February 2015 / Revised: 15 June 2015 / Accepted: 19 June 2015 / Published online: 2 July 2015  
© Springer Science+Business Media New York 2015

**Abstract** The timing of transmitter release from nerve endings is considered nowadays as one of the factors determining the plasticity and efficacy of synaptic transmission. In the neuromuscular junction, the moments of release of individual acetylcholine quanta are related to the synaptic delays of unquantal endplate currents recorded under conditions of lowered extracellular calcium. Using Bayesian modelling, we performed a statistical analysis of synaptic delays in mouse neuromuscular junction with different patterns of rhythmic nerve stimulation and when the entry of calcium ions into the nerve terminal was modified. We have obtained a statistical model of the release timing which is represented as the summation of two independent statistical distributions. The first of these is the exponentially modified Gaussian distribution. The mixture of normal and exponential components in this distribution can be interpreted as a two-stage mechanism of early and late periods of phasic synchronous secretion. The parameters of this distribution depend on both the stimulation frequency of the motor nerve and the calcium ions' entry conditions. The second distribution was modelled as quasi-

uniform, with parameters independent of nerve stimulation frequency and calcium entry. Two different probability density functions for the distribution of synaptic delays suggest at least two independent processes controlling the time course of secretion, one of them potentially involving two stages. The relative contribution of these processes to the total number of mediator quanta released depends differently on the motor nerve stimulation pattern and on calcium ion entry into nerve endings.

**Keywords** Neuromuscular junction · Quantal release of neurotransmitter · Kinetics of quantal secretion · Statistical model, Bayesian method

## Abbreviations

TCS	Time course of secretion
EPC	Endplate current
EMG	Exponentially modified Gaussian
$[Ca^{2+}]_{out}$	Extracellular calcium concentration
$[Mg^{2+}]_{out}$	Extracellular magnesium concentration
4-AP	4-aminopyridine
QU	Quasi-uniform process

Action Editor: Catherine E. Carr

✉ Ellya Bukharaeva  
elbukhara@gmail.com

<sup>1</sup> Kazan Federal University, Kremlevskaya St. 18, Kazan 420008, Russia

<sup>2</sup> Laboratory of the Biophysics of Synaptic Processes, Kazan Institute of Biochemistry and Biophysics, Russian Academy of Sciences, P.O. Box 30, Kazan 420111, Russia

<sup>3</sup> Kazan National Research Technical University named after A. N. Tupolev, K. Marx St. 10, Kazan 420111, Russia

<sup>4</sup> Kazan State Medical University, Butlerov St. 49, Kazan 420012, Russia

## 1 Introduction

The neuromuscular junction, a specialized area of contact between the axon terminal of a motor neuron and a muscle fibre, has been the subject of a wide range of neurophysiological studies. The mechanisms underlying neurosecretion are common to those of the fast chemical synapses of the central nervous system (Tarr et al. 2013). Under normal physiological conditions, the arrival of the action potential at the nerve ending triggers the secretion of up to several tens of quanta of

acetylcholine in the process known as phasic synchronous release (Katz 1996). In the period between nerve action potential and the moment of release of the individual synaptic vesicle, which is called a synaptic delay (or latency), a complicated multistage process takes place in the active zone involving several molecular complexes that are bound to both the presynaptic membrane and to the synaptic vesicle (Lin and Farber 2002; Pang and Sudhof 2010).

The duration of this process determines the latencies of single release events, and their distribution is the time course (or kinetics) of secretion (TCS) (Katz and Miledi 1965; Barrett and Stevens 1972; Nikolsky et al. 2004; Bukharaeva et al. 2007; Minneci et al. 2012). In the neuromuscular junction, phasic quanta release is started through 0.3–0.5 ms after the nerve action potential. It lasts several milliseconds and is not absolutely synchronous (Van der Kloot 1988b; Chang and Mennerick 2010).

Then the so-called delayed asynchronous secretion of neurotransmitter is observed after the nerve action potential and phasic quanta release. It has a duration of tens to hundreds of milliseconds and a rate about 1–5 % of that of phasic secretion (Rahamimoff and Yaari 1973; Atluri and Regehr 1998). It has been suggested that delayed asynchronous secretion is associated with the accumulation of calcium ions in the axoplasm, particularly at high firing frequencies (Hagler and Goda 2001; Feldchyshyn and Wang 2007; Smith et al. 2012).

There is also the intermediate component of quantal release which is observed 3–8 ms after the action potential (Chen and Regehr 1999; Gilmanov et al. 2008). This component is referred to as the late phasic release (Barrett and Stevens 1972; Bukharaeva et al. 2007) since these quanta can still take part in the formation of the integral endplate current (Van der Kloot 1988a, b). We have previously shown that, at the mouse neuromuscular junction, a decrease in the concentration of extracellular calcium results in the desynchronization of the neurosecretion process, due to the increased number of quanta released in the late period of phasic secretion (Bukharaeva et al. 2007).

Although both the phasic and delayed asynchronous secretion processes have been studied for a long time at different synapses (Rahamimoff and Yaari 1973; Goda and Stevens 1994; Atluri and Regehr 1998; Wen et al. 2013; Kaeser and Regehr 2014), precise mechanisms determining the timing of these release components and their dependence on calcium metabolism into nerve endings are not yet fully understood. There is a competition between the phasic and asynchronous release in developing hippocampal autaptic synapses (Otsu et al. 2004). Studies of excitatory autaptic currents evoked by single or repetitive stimulation from island cultures of hippocampal neurons have shown that phasic depression correlates with increased asynchronous quanta release (Chang and Mennerick 2010). Recently we found that at the neuromuscular junction of infant rats (6 and 10 days after birth) there is a

marked asynchronous phase of quantal release, along with a reduced number of quanta compared to the synapses of adults (Khuzakhmetova et al. 2014). The intensity of delayed asynchronous release in infants increased with the frequency of stimulation more than in adults. A blockade of the ryanodine receptor in the endoplasmic reticulum which can contribute to the formation of delayed asynchronous release in adults had no effect on the kinetics of delayed secretion in the infants unlike synapses of adult rats (Khuzakhmetova et al. 2014).

Thus, evidences has accumulated which suggests that phasic synchronous and delayed asynchronous release events are controlled by different mechanisms (Chung and Raingo 2013; Wen et al. 2013; Kaeser and Regehr 2014). However, it is unclear whether these processes are dependent or independent of each other.

In this connection, methods of statistical modelling can serve to describe the temporal parameters of the neurosecretion process because, in contrast to exact mathematical models, they do not require a detailed description of the process as a chain of biochemical reactions, a description that is not always possible due to the lack of experimental data.

Stevens (1968), and subsequently Bennett and Kearns (2000), applied this approach to analyse the distribution of real synaptic delays of release events forming the multiquantal response. The model suggested by these authors described well the temporal parameters of phasic secretion from extended amphibian and crayfish synapses at low ambient temperature, whereas delayed asynchronous secretion was not taken into consideration at all.

The purpose of the present study was to choose a statistical model to describe as well as possible the distribution of the real synaptic delays of unquantal endplate currents (EPCs) recorded at the mouse neuromuscular junction in 50 ms time frames following the stimulation artefact. The modelling aimed to provide answers to the following questions: (i) is the distribution of synaptic delays uniform or compound? (ii) if several components are involved in this distribution, are they mutually dependent? (iii) how do the parameters of the distribution(s) depend on the pattern of nerve firing and the various conditions governing the entry of calcium ions into the nerve terminal (namely, the gradient of  $\text{Ca}^{2+}$  concentration, the blocking of calcium channels, and the modification of the shape of the action potential)?

## 2 Material and methods

### 2.1 Electrophysiology

Experiments were performed on isolated mice phrenic nerve–diaphragm preparations. Mice (BALB/c strain) of both sexes of 20–25 g body weight were euthanized in accordance with the regulations of the European Community Council Directive

(September 22, 2010; 2010/63/EEC). The animal experiments were approved by the Ethical Committee of the Kazan State Medical University. The neuromuscular preparation, having been pinned to the bottom of the recording chamber, was continuously rinsed with the solution containing (all in mM): 150.0 NaCl, 5.0 KCl, 0.2–0.5 CaCl<sub>2</sub>, 5.0 HEPES, 5.0 MgCl<sub>2</sub>, and 11 glucose, with a pH of 7.3–7.4. Since the analysis of real synaptic delays reflecting the timing of secretion requires the selection of unquantal EPCs only (Katz and Miledi 1965), a modified Ringer's solution with extracellular calcium concentration  $[Ca^{2+}]_{out}$  reduced to 0.2–0.5 mM, and a magnesium concentration enhanced to 5 mM was used.

All experiments were performed at a temperature of 20.0±0.3 °C, and maintained using Peltier elements. The suction electrode was used to stimulate the motor nerve with supramaximal rectangular impulses of 0.2 ms duration and with stimulating frequencies of 0.5, 4, 10, and 15 Hz. The motor nerve action potentials and endplate currents were registered extracellularly with Ringer-filled glass micropipettes of tip diameter 2–3 μm and resistance 1.0–3.0 MΩ. The duration of the data frames was 50 ms, beginning from the onset of the stimulation artefact.

From 300 to 500 unquantal events were recorded, digitized at the sampling frequency of 3 μs, and analysed offline using software developed in our laboratory.

To exclude multiquantal responses from consideration, histograms of EPC amplitudes were drawn up, and only signals forming the first peak of the histogram were selected for subsequent analysis of the real synaptic delays, as previously described (Bukcharaeva et al. 1999; Bukcharaeva et al. 2002).

The synaptic delays were estimated as the time intervals from the nerve sodium spikes to the early (20 % of maximum amplitude) phase of the EPC (Bukcharaeva et al. 1999; Bukcharaeva et al. 2007). Following that delay, histograms of the unquantal EPCs were plotted. The mean value of the shortest 5 % of synaptic delays in each series was taken as the minimal synaptic delay (Barrett and Stevens 1972).

In addition to  $[Ca^{2+}]_{out}$  variation (ranging from 0.2 to 0.5 mM), the blocker of voltage-sensitive Ca<sup>2+</sup> channels 2.5 μM cadmium chloride (Dudel et al. 1991) and the potassium channels blocker 5 μM 4-aminopyridine (Muller 1986) were used to modify the conditions of calcium ion entry into the nerve endings.

All chemicals were purchased from Sigma.

## 2.2 Statistical modelling

The standard procedure of Bayesian modelling, well described in the literature (Matzke et al. 2013; Gelman et al. 2014), was used to model the probability density function of the synaptic delays of unquantal EPCs.

Different two-component mixture distributions (with components corresponding to the main peak and background) and

three-component mixture distributions (with main peak, second peak, and background) were considered. The components were selected on the basis of the form of the histogram of the experimentally obtained latencies, and of previously reported data testifying to the three phases of secretion varying by rates of release (Chen and Regher 1999).

Normal, log-normal, shifted gamma, and exponentially modified Gaussian (EMG) distributions were tested as the main peak distributions, while distributions that were uniform, exponentially decaying, and with density inversely proportional to time were used to describe the background process.

The *rjags* program (Plummer 2012) and the R package *R2jags* (Su and Yajima 2012) were used for the model fitting. Calculations were performed in five independent realizations (chains) with randomly selected initial parameters. Four thousand steps were taken to initialize the distribution, followed by another two thousand steps to obtain the sample of the model parameters. Each fifth value was included in the sample to avoid autocorrelation. Thus, the size of the total sample of five chains was 2000 values for each model parameter. According to the convergence criteria, the parameter distributions should be the same for all chains, which suggested that the results tended toward the stationary distribution. In theory, such distribution should asymptotically approach the true distribution of the model parameters fitting the experimental data.

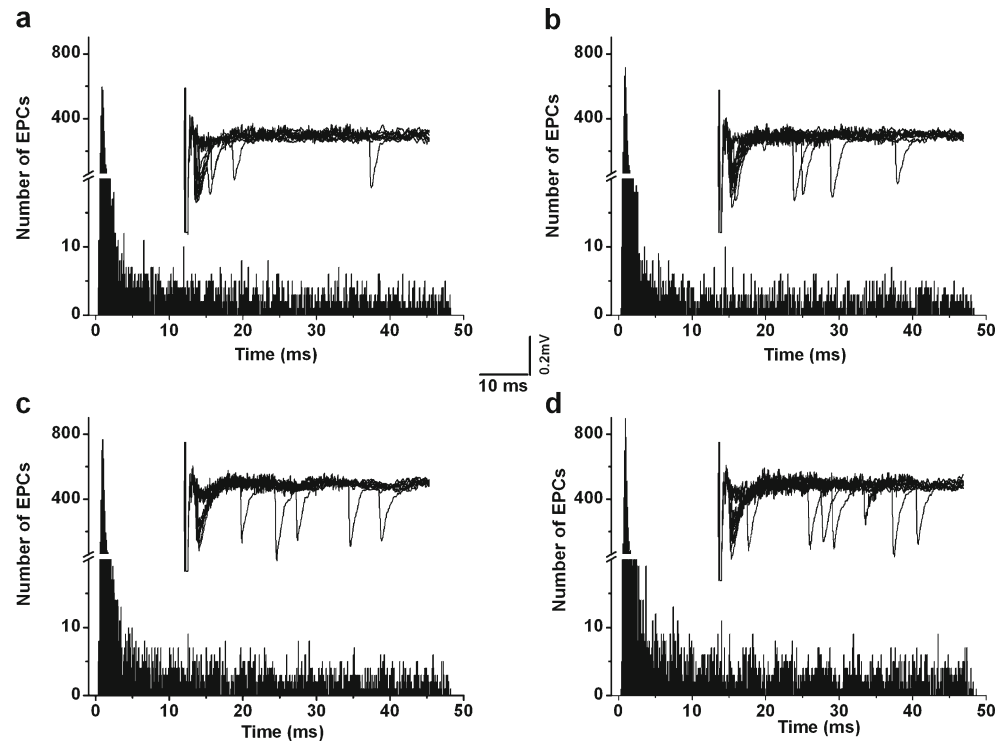
## 3 Results

### 3.1 Electrophysiological studies

Under control conditions ( $[Ca^{2+}]_{out}=0.5$  mM,  $[Mg^{2+}]_{out}=5$  mM), nerve stimulation (0.5 Hz) evoked nerve action potentials, followed by EPCs (of mean quantal content  $0.47\pm 0.05$ ) with significantly varying latencies of the unquantal responses (Fig. 1a, inserts). The majority of EPCs had short delays of up to 3 ms after the peak of the sodium component of nerve action potential, corresponding to the phasic synchronous release (Katz and Miledi 1965; Goda and Stevens 1994; Augustine 2003). Significantly fewer EPCs occurred in the next 47 ms of recording; these were events characterized as delayed asynchronous secretion (Rahamimoff and Yaari 1973; Chen and Regher 1999). Correspondingly, the distribution histogram of real synaptic delays had a marked peak formed by quanta released in the first 3 ms (synchronous release) and an extended “tail” made up of long-latency events – delayed asynchronous release (Fig. 1a). Higher stimulation frequencies resulted in increased intensity of both synchronously and asynchronously released quanta (Fig. 1b–d).

When the level of extracellular calcium (and, correspondingly, the concentration gradient) has decreased from 0.5 to 0.3 and 0.2 mM, the calcium current through voltage-sensitive channels should diminish. As a result, the total number of

**Fig. 1** Kinetics of quantal release under different frequencies of nerve stimulation. **a** Histograms of real synaptic delays distribution of EPCs and 10 randomly selected trails (insert) recorded at 0.5 Hz nerve stimulation ( $[Ca^{2+}]_{out}=0.5$  mM), the total number of EPCs is 4785; **b** at 4 Hz, the total number of EPCs is 5226; **c** at 10 Hz, the total number of EPCs is 5719; **d** at 15 Hz, the total number of EPCs is 6447. Total number of stimuli is 10000 in 8 synapses



quanta secreted was lower, though to different extents for release events that occurred with small latencies (in the synchronous phase) and for delayed releases (in the asynchronous phase following the main mode of distribution) (Fig. 2a and c).

Higher stimulation frequencies at lower calcium levels also resulted in greater release intensities. However, a direct comparison of the delay histograms does not allow accurate estimation of the changes in intensities of both synchronous and delayed asynchronous secretions (Fig. 2b and d).

When voltage-sensitive calcium channels were blocked by cadmium ions, the number of secreted mediator quanta was also reduced, compared to the control  $[Ca^{2+}]_{out}=0.5$  mM, due to the lower calcium entry (Fig. 2e and f).

The application of the potassium channel blocker 4-AP (Muller 1986) led to a prolonged depolarization phase of nerve action potential, and consequently, to enhanced  $Ca^{2+}$  entry into the nerve endings. Under these conditions, the number of synchronously released quanta increased to a greater degree (Fig. 2g and h; these experiments were performed at  $[Ca^{2+}]_{out}=0.3$  mM, and therefore were compared to recordings made at this calcium level).

Thus, an analysis of release timing made on the basis of the conventional separation of uniquantal EPCs into synchronous (occurring 3 ms after nerve action potential) and delayed asynchronous (from 3 to 50 ms after nerve action potential) events suggested that the intensity of these processes depends in different ways on the stimulation frequency and on the manner of modulation of calcium entry into the nerve endings.

The statistical model of the distribution of synaptic delays was developed to quantitatively estimate changes in TCS induced by experimental manipulations and to separate specific components (e.g., the early and delayed-release events) that form the resulting secretion.

### 3.2 Statistical model

The results of Bayesian simulation of the mixture distribution of synaptic delays show that only the most trivial two-component mixture model based on the EMG distribution for the main peak and quasi-uniform background distribution (for EPCs with latencies longer than the value of the main mode of the histogram) appeared to be numerically stable across the whole body of experimental data and to fit them well. All other models appeared to be numerically unstable.

The probability density function for the EMG distribution was modelled as convolution:

$$f(t|\mu, \sigma, \lambda) = \left( \left( \frac{\lambda}{\sigma \cdot \sqrt{2 \cdot \pi}} \right) \cdot e^{-\frac{(\mu-t)^2}{2 \cdot \sigma^2}} \right) * (e^{-\lambda \cdot t}), \quad (1)$$

where  $\mu$  is the mean of the Gaussian,  $\sigma^2$  is the variance of the Gaussian, and  $\lambda$  is the rate of exponential component decay.

All attempts to replace EMG by other density functions, or to add one more distribution to simulate the “intermediate” process corresponding to latencies of 3

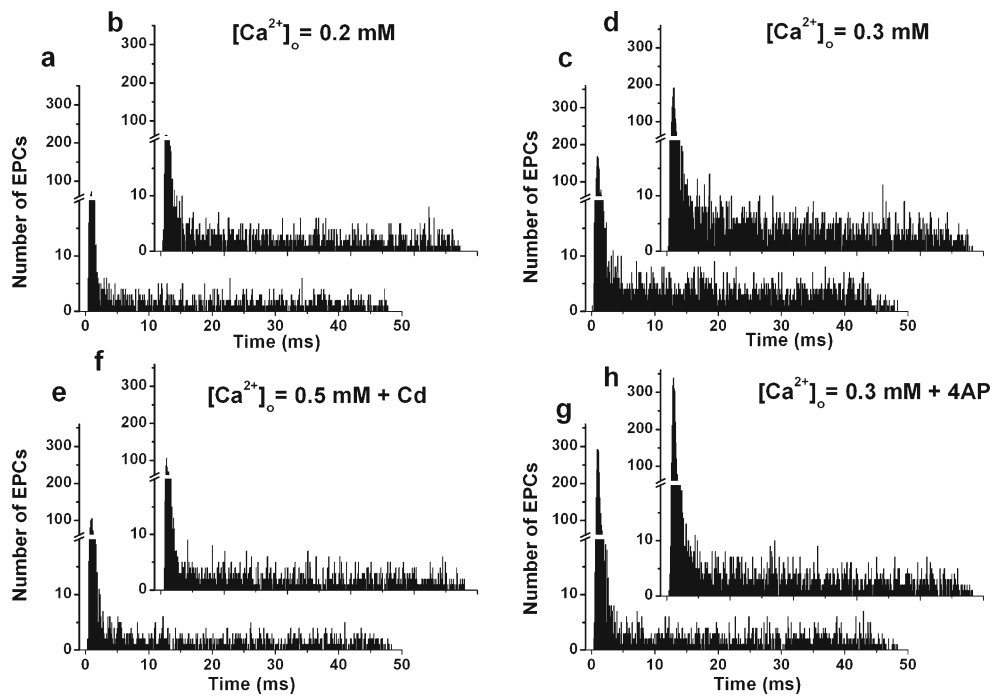


**Fig. 2** Kinetics of quantal release under modified calcium entry into the nerve ending. Histograms of distribution of real synaptic delays of EPCs recorded under modified calcium entry into nerve ending. **a**  $[Ca^{2+}]_{out}=0.2$  mM, 0.5 Hz nerve stimulation, the total number of EPCs is 1203; **b**  $[Ca^{2+}]_{out}=0.2$  mM, 15 Hz nerve stimulation, the total number of EPCs is 1617; **c**  $[Ca^{2+}]_{out}=0.3$  mM, 0.5 Hz nerve stimulation, the total number of EPCs is 3017; **d**  $[Ca^{2+}]_{out}=0.3$  mM, 15 Hz nerve stimulation, the total

number of EPCs is 3566; **e** in presence of 2.5  $\mu$ M cadmium, 0.5 Hz nerve stimulation, the total number of EPCs is 1534; **f** in presence of 2.5  $\mu$ M cadmium, 15 Hz nerve stimulation, the total number of EPCs is 1672; **g** in presence of 5  $\mu$ M 4-AP, 0.5 Hz nerve stimulation, the total number of EPCs is 3151; **h** in presence of 5  $\mu$ M 4-AP, 15 Hz nerve stimulation, the total number of EPCs is 3957. Total number of stimulus is 10000 in 8 synapses for each series

to 8 ms (Chen and Regher 1999), made the model numerically unstable because of the small “package” of latencies found in each record; these were close to each other for the particular synapse, but different from one experiment to another (under the same recording conditions, such as  $[Ca^{2+}]_{out}$ , pattern of nerve firing, drug applications, etc.).

The model probability density function  $f(t_{i,j,k})$  of the observed latencies  $t_{i,j,k}$  (where  $k$  is the index number of the latency recorded in the  $j^{th}$  experiment with the  $i^{th}$  set of parameters), is represented as:

$$f(t_{i,j,k}) = p_{i,1} \cdot f_1(t_{i,j,k} | \mu_{i,j}, \sigma, \lambda_{i,j}) + p_{i,2} \cdot f_2(t_{i,j,k} | x_{min}, x_{max}, \nu(a_0, a_1, t_{i,j,k})), \quad (2)$$

This provided the best fit to the experimental data in the context of both the reproducibility and the likelihood function.

Here,  $f_1(t_{i,j,k} | \mu_{i,j}, \sigma, \lambda_{i,j})$  is the probability density function of the EMG distribution with mean  $\mu_{i,j}$ , standard deviation  $\sigma$  (in our model, a constant parameter equal to 121.274  $\mu$ s), and the rate  $\lambda_{i,j}$ , describing the distribution of the fast (early) latencies of the synchronously released mediator quanta in the  $j^{th}$  experiment with the  $i^{th}$  set of parameters.

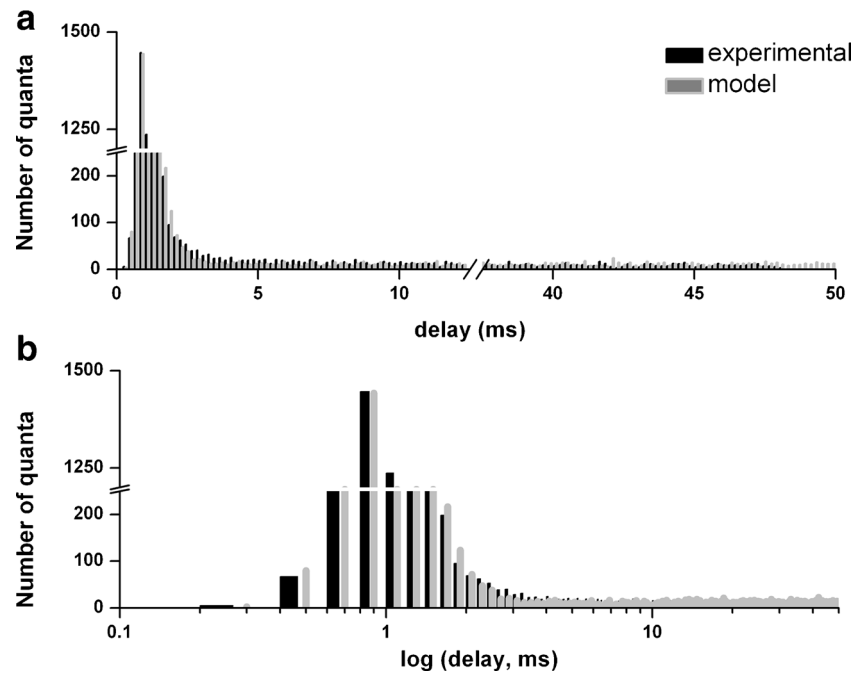
Next,  $f_2(t_{i,j,k} | x_{min}, x_{max}, \nu(a_0, a_1, t_{i,j,k}))$  is the probability function of the second distribution, which is almost uniform on  $[x_{min}, x_{max}]$ , with density dependent on time. The latter is presented as  $f_2(t_{i,j,k} | x_{min}, x_{max}, \nu(a_0, a_1, t_{i,j,k})) = \frac{1}{Z} \cdot \frac{1}{\nu(a_0, a_1, t_{i,j,k})}$ , where  $Z$  is a normalizing factor.  $Z = \frac{1}{a_1} \cdot \ln\left(\frac{\nu(a_0, a_1, X_{max})}{\nu(a_0, a_1, X_{min})}\right)$ , and in the range  $[x_{min}, x_{max}] = [400, 50000]$ ,  $Z$  is equal to 260.

Furthermore,  $\nu(a_0, a_1, t_{i,j,k})$  is the dependence of the mean time interval between adjacent pulses on the time since the stimulation artefact. In particular, in our model,  $\nu(a_0, a_1, t_{i,j,k}) = a_0 + a_1 \cdot t$ , where  $a_0 = 123.845$  (s.d. = 10.671),  $a_1 = 3.077 \cdot 10^{-3}$  (s.d. =  $0.282 \cdot 10^{-3}$ );  $p_{i,1}, p_{i,2}$  are mixing probabilities ( $p_{i,1} + p_{i,2} = 1$ ).

Figure 3 compares the total experimental histogram of the latencies obtained in eight neuromuscular junctions stimulated at 0.5 Hz ( $[Ca^{2+}]_{out} = 0.5$  mM) with the sample from the distribution with the fitted parameters. Although the mixture of two distributions described above sufficiently closely matched the experimentally obtained data, some patchy deviations were nonetheless observed; these may be accounted for by the heterogeneity of experimental material.

The model assumed that the parameter  $\mu_{ij}$  includes a constant part that is invariant across all experiments and under all conditions, and a variable component that depends on the

**Fig. 3** Experimental and model distributions of synaptic delays. Experimental (*black columns*) and model (*gray columns*) histograms of real synaptic delays of EPCs at 0.5 mM  $[Ca^{2+}]_{out}$  and 0.5 Hz stimulation frequency. **a** Linear time scale (note the break on the abscissa axis between 13.5 and 37.5 ms); **b** logarithmic time scale for better representation of the main peak



particular recording and its condition. Interestingly, the logarithm of this parameter turned out to be linearly dependent on the stimulation frequency, so the following equation was used in the simulation:

$$\ln(\mu_{ij}) = \mu_0 + \beta_{m(i)} + \gamma \cdot Freq(i), \quad \text{with } \gamma = \gamma_0 + \gamma_{m(i)}, \quad (3)$$

where  $\mu_0$  is the constant component,  $\beta_{m(i)}$  is the contribution of the particular experimental condition  $m(i)$ , and  $\gamma$  is a coefficient related to the contribution of the stimulation frequency  $Freq(i)$ , involving constant ( $\gamma_0$ ) and experimentally determined ( $\gamma_{m(i)}$ ) parts. These components are different from zero when the influence of experimental conditions is significant.

Similarly, it was suggested that

$$\lambda_{i,j} = \lambda_0 + \delta_{m(i)} + (\tau_0 + \tau_{m(i)}) \cdot Freq(i), \quad (4)$$

with corresponding coefficients indicating the contribution of experimental conditions and stimulation frequencies to the rate  $\lambda_{ij}$ . This parameter itself was linearly dependent on stimulation frequency.

For all the models but this one the Gelman-Rubin convergence diagnostic (Gelman and Rubin 1992) indicates lack of convergence (statistical values substantially above 1, up to an order of magnitude for some model parameters), and parameter distribution graphs display different forms for distinct chains.

We sampled from the modelled latency distributions obtained from the 0.5, 4, 10, and 15 Hz stimulations and at three different calcium levels ( $[Ca^{2+}]_{out}$  at 0.5, 0.3, and 0.2 mM for each frequency). For each stimulation frequency we also

modelled the changes in the histogram in the presence of cadmium which is known to diminish  $Ca^{2+}$  entry into nerve endings, and in the presence of 4-AP to extend the period of calcium entry due to repetitive channel opening. The calcium concentration of 0.5 mM was selected as the reference condition for the estimation of statistical significance of experimental impacts. All pairwise differences were significant at the 95 % level.

The pooled results for the different recording conditions and stimulation frequencies related to  $\mu$  and  $\tau$  (decay time constant of the exponential part of EMG,  $\tau = 1/\lambda$ ) are given in Table 1 and in Figs. 4 and 5. Note that the parameter  $\mu$  defines the total shift of latencies on a temporal scale, whereas  $\tau$  is responsible for the proportion of events that markedly exceed the mean value of the main mode of the histogram.

Our statistical model permitted us to evaluate the contribution of each of the described processes in the total number of release events, and the dependence of this proportion on the recording conditions. Our calculations have shown that the proportion of the first (EMG) process in the pool of all latencies depended strongly on calcium concentration in the nerve ending (Fig. 6) and weakly on the stimulation frequency. Each rectangle in Fig. 6 corresponds to the 25 to 75 % range of latencies, with horizontal bars indicating mean values and error bars related to the 2.5 to 97.5 % range of all events. As can be seen from Fig. 6, the attenuation of the intensity of the two-stage EMG process that occurred at decreased calcium entry into the nerve endings was achieved in different ways (decreased  $[Ca^{2+}]_{out}$  or by cadmium blocking the calcium channels). At the same time, enhanced calcium entry under conditions of elevated extracellular  $[Ca^{2+}]_{out}$  or in the

**Table 1** Dependence of model parameters (Eqs. 3 and 4) on stimulation frequency and experimental conditions ( $[Ca^{2+}]_{out}=0.2-0.5$  mM). Values of  $\tau$ ,  $\lambda$  and  $\delta$  are in  $1/\mu s$ ; values  $\beta$ ,  $\gamma$  and  $\mu_0$  are on log time scale;  $\mu_0 = 6.7$

Substance	$\beta_{m(i)}^{(1)}$	$\gamma_0^{(1)} + \gamma_{m(i)}^{(1)}$	$\lambda_0^{(1)} + \delta_{m(i)}^{(1)}$	$\tau_0^{(1)} + \tau_{m(i)}^{(1)}$
4-AP	0.0519	0.00376	0.00270	0.0000188
$[Ca^{2+}]_{out}=0.2$	-0.0532	-0.00108	0.00338	-0.0001077
$[Ca^{2+}]_{out}=0.3$	-0.0646	0.00411	0.00239	0.0000011
$[Ca^{2+}]_{out}=0.5$	-0.0723	0.00874	0.00321	0.0000142
Cadmium	-0.0654	0.00580	0.00285	-0.0000522

presence of 4-AP (prolonging the presynaptic action potential) resulted in an increase of this process’s contribution to the pool of all release events. The averaged calculated number of EPCs in each of two main components, EMG and quasi-uniform (QU), under different experimental conditions are given in Table 2.

### 4 Discussion

The analysis of neurotransmitter secretion timing has attracted increasing attention from many researchers in recent years (Hagler and Goda 2001; Neff et al. 2009; Chang and Mennerick 2010; Wen et al. 2013; Kaeser and Regehr 2014). The kinetics of quantal release at chemical synapses is critical for determining synaptic efficacy because it modulates the amplitude and the temporal characteristics of multiquantal postsynaptic signals (Fesce 1999; Sabatini and Regehr 1999). The fluctuations in EPC delays, defined as the time interval between nerve stimulation and the beginning of the response, are due to the statistical nature of presynaptic, time-dependent, probabilistic processes governing evoked quantal release (Katz and Miledi 1965; Barrett and Stevens 1972). Apart from this, the detailed study of temporal

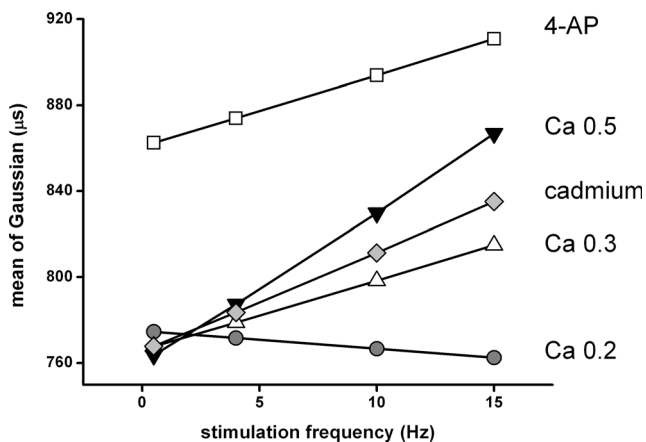


**Fig. 4** Dependence of the parameter  $\mu$  on the stimulation frequency at modified calcium entry conditions

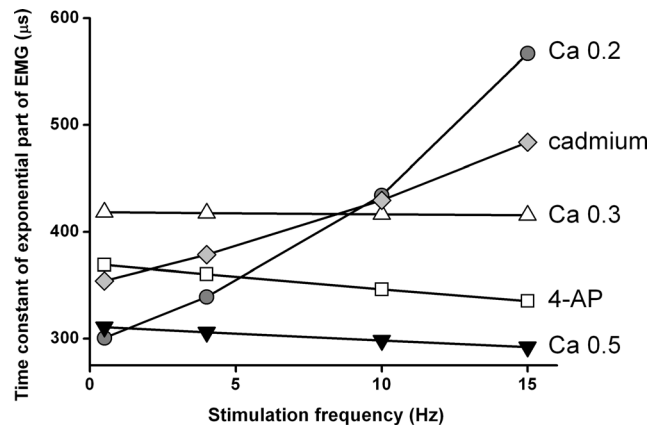


**Fig. 5** Dependence of the parameter  $\tau(I/\lambda)$  on the stimulation frequency at modified calcium entry conditions

parameters of the release process allows us to suggest the existence of at least three modes of quantal secretion: spontaneous, evoked synchronous, and evoked delayed asynchronous (Wen et al. 2013; Kaeser and Regehr 2014). The physiological role of synchronous neurotransmitter release is clear enough, while the significance of spontaneous and delayed asynchronous secretion is not fully understood. At most synapses, the asynchronous secretion is smaller than the synchronous one, but it becomes more prominent with repetitive stimulation (Atluri and Regehr 1998; Lu and Trussel 2000; Hefft and Jonas 2005).

The conventional direct method of evaluation of the secretion time frames based on the comparison of histograms of real synaptic delays (Katz and Miledi 1965; Barrett and Stevens 1972) does not allow precise estimation of the character of the change in the release kinetics under varying experimental conditions. Moreover, the distribution of real synaptic delays is not Gaussian, which means it would be improper to use the mean value as an estimate.

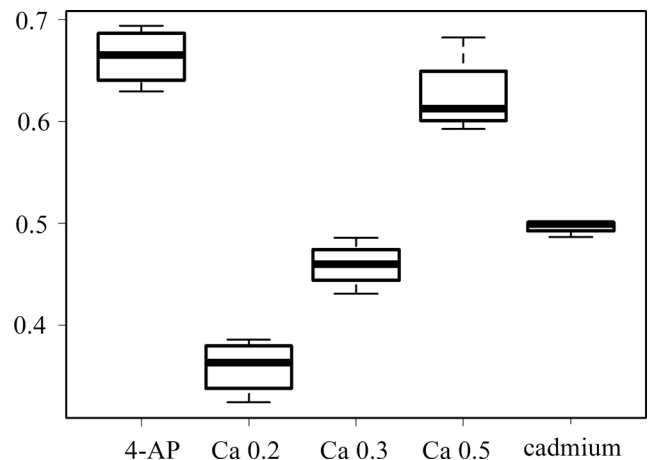


**Fig. 6** Dependence of EMG contribution to the total number of responses on experimental conditions. Each rectangle shows the range from 25 to 75% of all the signals, the horizontal bar within each rectangle is related to the mean value, error bars show the range from 2.5 to 97.5% of all signals

**Table 2** Most likely number of EPCs in each of two main components, EMG and quasiuniform (QU), under different experimental conditions, data are calculated as the product of corresponding probabilities and total amount of EPCs in a particular set of experiments

Experimental protocol	0.5 Hz		4 Hz		10 Hz		15 Hz	
	EMG	QU	EMG	QU	EMG	QU	EMG	QU
4-AP	145	65	151	63	152	77	169	94
[Ca <sup>2+</sup> ] <sub>out</sub> =0.2	73	143	71	108	93	135	124	185
[Ca <sup>2+</sup> ] <sub>out</sub> =0.3	91	110	96	100	107	108	119	119
[Ca <sup>2+</sup> ] <sub>out</sub> =0.5	171	111	196	87	209	124	229	141
Cadmium	111	109	103	101	132	133	139	139

In the present study, we performed statistical modelling to quantitatively characterize the distributions of synaptic delays of unquantal EPCs recorded in mouse neuromuscular junctions under different experimental conditions. The statistical model answered some questions on the nature of the processes that determine the timing of the release of mediator quanta from nerve endings following presynaptic action potential arrival.

The non-physiological, low calcium concentration was used for a special purpose to detect different mechanisms of neurotransmitter release. In vertebrate neuromuscular junctions fast synchronous release of neurotransmitters dominates at the physiological calcium level (Van der Kloot 1988b). Special mathematical tools have to be applied to evaluate the moments of single quanta secretion (Van der Kloot 1988a; Gainulov et al. 2002). However, our early studies showed that even at the physiological calcium level the release was not fully synchronous, and the delayed asynchronous release declined but did not disappear (Bukharaeva et al 2007). Since the delayed asynchronous release does not participate in ECP formation but plays some other roles (e.g., modulatory one), then even a few delayed quanta can be important for synapse functioning (Kaesler and Regehr 2014). Moreover, during natural activity, e.g., at 20–100 Hz synapse activation, the contribution of asynchronous release may be increased.

The statistical analysis of the synaptic delays distribution by Bayesian modelling showed that the secretion process is made up of at least two independent mechanisms following essentially different stochastic laws. Notably, one of these processes involves two components, as it can be described as the convolution of Gaussian and exponential probability density function (EMG). The first component of this process is accounting for the main peak of the latency histogram, equal to approximately 1 ms (specifically,  $0.82 \pm 0.02$  ms, depending on the individual properties of the neuromuscular preparations) and can be mostly described by the normal probability density function. This component can be considered as the early period of the synchronous phasic release, as has been suggested previously (Barrett and Stevens 1972; Goda and Stevens 1994; Wen et al. 2013). During this period, neurotransmitter quanta are released with low temporal dispersion.

The parameter  $\mu$  in the EMG is related to the shift of synaptic delays on the time scale, i.e., to the mode of the

histogram, and includes an invariant part  $\mu_0$  (see Eq. 3). According to our model calculations,  $\mu_0$  provides a delay  $0.67 \pm 0.02$  ms. One would assume that  $\mu_0$  is the so-called minimal synaptic delay (Katz and Miledi 1965; Bukharaeva et al. 2007). The experimentally estimated minimal synaptic delay in our experiments equals  $0.63 \pm 0.02$  ms ( $n=32$ ), and does not depend on the extracellular [Ca<sup>2+</sup>]<sub>out</sub> value (Barrett and Stevens 1972; Bukharaeva et al. 2007). However, the prolongation of the repolarization phase of the presynaptic membrane in the presence of 4-AP resulted in an increase of the minimal synaptic delay up to  $0.71 \pm 0.03$  ms (paired *t*-test,  $p < 0.05$ ,  $n=30$ ) in experiments with enhanced stimulation frequency (15 Hz) and [Ca<sup>2+</sup>]<sub>out</sub>=0.5 mM. Therefore,  $\mu_0$  cannot be fully equated to the minimal synaptic delay which actually depends slightly on a number of experimental conditions.

Figure 4 shows that at 0.5 Hz nerve stimulation parameter  $\mu$  is practically the same for different calcium concentrations and in the presence of cadmium blocking the entry of calcium into the nerve ending. But the statistical model revealed the significant increase of  $\mu$  for high frequency stimulation conditions. This manifested itself most vividly at enhanced calcium entry into the nerve terminal in the presence of 4-AP ([Ca<sup>2+</sup>]<sub>out</sub>=0.3 mM). The increase of  $\mu$  by 12 % was revealed for this condition. Possible explanations of such an increase can be the elevation of calcium entry after blocking of potassium channels and activation of distant calcium channels by broad action potential (Vyshedskiy and Lin 2000). Moreover, according to the other data, the rate parameters of calcium channel activation and inactivation are assumed to be voltage-dependent (Bennett et al. 1997; Delcour et al. 1993). Therefore, even the initial part of the latency distribution can follow the changes in the shape of the presynaptic spike and, as in the case of 4-AP, may be different from control conditions. Varying Ca<sup>2+</sup> influx when release is probed with broad action potential permits detection of changes in synaptic delay resulting from even small variations in local [Ca<sup>2+</sup>]<sub>in</sub> (Lin and Farber 2002; Vyshedskiy and Lin 2000).

When, in contrast, calcium entry was reduced by the voltage-sensitive calcium channel blockage by cadmium ions and at the decreased (down to 0.2 mM) level of extracellular Ca<sup>2+</sup>, this dependence on stimulation frequency was attenuated (Fig. 4). The change in  $\mu$  at enhanced motor nerve



stimulation frequency testifies to the extended interval between the peak of the sodium component of the action potential and the time when the maximal number of quanta are released.

The second phase of the EMG process following the exponential law with decay time constant  $\tau = 1/\lambda$  also depends on both the stimulation frequency and the calcium level (Table 1). Fig. 5 shows that an increase in the stimulation frequency resulted in a twofold increase of  $\tau$  under conditions of decreased  $[Ca^{2+}]_{out}$  (to 0.2 mM) and when calcium channels were blocked by cadmium. This coincides with the experimentally observed increase in the asynchrony of the late period of secretion at high frequency firing in both the central and peripheral synapses (Atluri and Regehr 1998; Lu and Trussel 2000; Hefft and Jonas 2005).

Thus, two components of the evoked release process following EMG distribution correspond to the early and late periods of phasic synchronous secretion with parameters depending on both nerve stimulation frequency and the conditions of calcium ion entry into the nerve ending. Both components contribute simultaneously to the total distribution of release latencies, and are associated directly with calcium entry in the proximity of the active zone of secretion, with localization of calcium channels in the active zone, and with mechanisms maintaining the intracellular calcium level at a high frequency of firing. It can be suggested that these components reflect the interaction of calcium entering the terminal with proteins coupled to ready-to-release synaptic vesicles docked close to the calcium channels which are activated by membrane depolarization. Three key factors are required to trigger synchronous release: vesicles that can be quickly released after  $Ca^{2+}$  entry; fast opening presynaptic voltage-gated  $Ca^{2+}$  channels with minimal delay upon arrival of the nerve action potential; close and rapid interaction between synaptic vesicle and  $Ca^{2+}$  sensor to trigger exocytosis (see rev. Kaeser and Regehr 2014). Each of these factors can have its own dependence on the pattern of stimulation of the motor nerve and conditions of entry of calcium ions and thereby determine the early and late phases of secretion. According to Parnas's calcium-voltage hypothesis, depolarization of the presynaptic terminal has two functions (Parnas and Parnas 2010). First, in common with the calcium hypothesis, the  $Ca^{2+}$  conductance is increased, thereby permitting  $Ca^{2+}$  entry. Second, a conformational change is induced in a membrane molecule that renders it sensitive to  $Ca^{2+}$ , and then binding of  $Ca^{2+}$  to this active form triggers release of neurotransmitter molecules. This hypothesis focuses attention on the initial 4–5 ms of the release process only (synchronous phase) since it is a period of changes in membrane potential induced by nerve activation. However, it can be used for the explanation of some of our results, especially those relating to the early phase of release (EMG process).

The statistical model revealed the background process with its parameters to be practically independent of experimental conditions (calcium entry and stimulation frequency). It may be suggested that the events attributed to this distribution are not triggered directly by calcium entry into the nerve ending from the synaptic cleft; instead they reflect the so-called delayed asynchronous quantal release (Rahamimoff and Yaari 1973; Atluri and Regehr 1998). Our model data does not show the dependence parameters of this release from calcium entry and stimulation frequency.

Studies of the  $Ca^{2+}$  dependence of vesicle fusion as written in the review by Kaeser and Regehr (2014) suggest that specialized  $Ca^{2+}$  sensors can mediate the asynchronous release. At the crayfish neuromuscular junction, a linear relationship between the frequency of quantal events and presynaptic  $Ca^{2+}$  levels was revealed when the  $Ca^{2+}$  concentration was less than 600 nM; a much steeper dependence on  $Ca^{2+}$  was found for higher levels of  $Ca^{2+}$  (Delaney and Tank 1994). At cerebellar granule cell synapses, a component of asynchronous release lasting hundreds of milliseconds was linearly dependent on  $Ca^{2+}$ , and a component lasting tens of milliseconds was more steeply dependent on  $Ca^{2+}$  (Atluri and Regehr 1998). These findings suggest that asynchronous release is mediated by a specialized  $Ca^{2+}$  sensor with a linear dependence on  $Ca^{2+}$ . A model of release with multiple  $Ca^{2+}$  sensors successfully accounts for asynchronous release at the crayfish neuromuscular junction (Pan and Zucker 2009).

The comparison of the fraction of release events making up the first (two-stage) process and the second quasi-uniform process under the conditions promoting calcium ions entry into the nerve ending (elevated  $[Ca^{2+}]_{out}$ , extended presynaptic action potential) indicates an increased contribution from the first (EMG) process (Fig. 6). That corresponds to the conventional experimental results demonstrating intensified phasic synchronous secretion at elevated calcium ion levels (Dodge and Rahamimoff 1967; Sabatini and Regehr 1999; Neher and Sakaba 2008; Dudel 2009). However, according to our experimental data, the proportion of release events governed by the EMG process was attenuated when the nerve stimulation frequency was increased. This indicates the increased contribution of the second (quasi-uniform) process, and is in agreement with the behaviour of the delayed asynchronous release demonstrating a reciprocal relation with synchronous release (Hagler and Goda 2001; Otsu et al. 2004; Neff et al. 2009).

However, the possibility that the unquantal events associated with the uniform distribution were, in fact, spontaneously released miniature EPCs must not be ruled out. To check this hypothesis, an additional comparison of the distributions of the interstimulus intervals of spontaneously occurring miniature and evoked unquantal EPCs recorded at the same synaptic contact would be required.

**Acknowledgments** Supported by the Russian Government's Program for Competitive Growth of Kazan Federal University and was also supported by a grant of President of Russian Federation "Leading Scientific School" and a grants from the Russian Foundation for Basic Research (13-04-00886 for DS; 14-04-00987 for IK and EN, 14-04-00790 for AS, 15-04-02983 for VKh and EB).

**Conflict of interest** The authors declare that they have no conflict of interest.

## References

- Atluri, P. P., & Regehr, W. G. (1998). Delayed release of neurotransmitter from cerebellar granule cells. *Journal of Neuroscience*, *18*(20), 8214–8227.
- Augustine, G. J. (2003). How does calcium trigger neurotransmitter release? *Current Opinion in Neurobiology*, *11*(3), 320–326.
- Barrett, E. F., & Stevens, C. F. (1972). The kinetics of transmitter release at the frog neuromuscular junction. *Journal of Physiology*, *227*, 691–708.
- Bennett, M. R., & Kearns, J. L. (2000). Statistics of transmitter release at nerve terminals. *Progress in Neurobiology*, *60*(6), 545–606.
- Bennett, M. R., Gibson, W. G., & Robinson, J. (1997). Probabilistic secretion of quanta and the synaptosecretosome hypothesis: evoked release at active zones of varicosities, boutons, and endplates. *Biophysical Journal*, *73*(4), 1815–1829.
- Bukharaeva, E., Samigullin, D., Nikolsky, E., & Vyskocil, F. (2002). Protein kinase A cascade regulates quantal release dispersion at frog muscle endplate. *Journal of Physiology*, *538*, 837–848.
- Bukharaeva, E. A., Samigullin, D. V., Nikolsky, E. E., & Magazanik, L. G. (2007). Modulation of the kinetics of evoked quantal release at mouse neuromuscular junctions by calcium and strontium. *Journal of Neurochemistry*, *100*, 939–949.
- Bukharaeva, E., Kim, K., Moravec, J., Nikolsky, E., & Vyskočil, F. (1999). Noradrenergic synchronizes evoked quantal release at frog neuromuscular junctions. *Journal of Physiology*, *517*, 879–888.
- Chang, C. Y., & Mennerick, S. (2010). Dynamic modulation of phasic and asynchronous glutamate release in hippocampal synapses. *Journal of Neurophysiology*, *103*, 392–401.
- Chen, C., & Regehr, W. (1999). Contributions of residual calcium to fast synaptic transmission. *Journal of Neuroscience*, *19*, 6257–6266.
- Chung, C., & Raingo, J. (2013). Vesicle dynamics: how synaptic proteins regulate different modes of neurotransmission. *Journal of Neurochemistry*, *126*(2), 146–154. doi:10.1111/jnc.12245.
- Delaney, K. R., & Tank, D. W. (1994). A quantitative measurement of the dependence of short-term synaptic enhancement on presynaptic residual calcium. *Journal of Neuroscience*, *14*(10), 5885–5902.
- Delcour, A. H., Lipscombe, D., & Tsien, R. W. (1993). Multiple modes of N-type calcium channel activity distinguished by differences in gating kinetics. *Journal of Neuroscience*, *13*(1), 181–194.
- Dodge, F., & Rahamimoff, R. (1967). Cooperative action of calcium ions in transmitter release at the neuromuscular junctions. *Journal of Physiology*, *193*, 419–432.
- Dudel, J. (2009). Depolarization amplitude and  $Ca^{2+}$ -inflow control the time course of quantal releases at murine motor nerve terminals. *European Journal of Neuroscience*, *30*(7), 1219–1226. doi:10.1111/j.1460-9568.2009.06915.x.
- Dudel, J., Parnas, H., & Parnas, I. (1991). Evoked phasic release in frog nerve terminals obtained after block of  $Ca^{2+}$  entry by  $Cd^{2+}$ . *Pflügers Archiv*, *419*(2), 197–204.
- Feldchyshyn, M. J., & Wang, L. Y. (2007). Activity-dependent changes in temporal components of neurotransmission at the juvenile mouse calyx of Held synapse. *Journal of Physiology*, *581*, 581–602.
- Fesce, R. (1999). The kinetics of nerve-evoked quantal secretion. *Philosophical Transactions of the Royal Society, B: Biological Sciences*, *354*, 319–329.
- Gainulov, R., Bukharaeva, E., & Nikolskii, E. (2002). A method for assessing the kinetics of evoked secretion of transmitter quanta determining the generation of multi-quantum endplate currents. *Neuroscience Behavioral Physiology*, *32*(6), 613–616.
- Gelman, A., & Rubin, D. B. (1992). Inference from iterative simulation using multiple sequences. *Statistical Science*, *7*, 457–511.
- Gelman, A., Carlin, J. B., Stern, H. S., Dunson, D. B., Vehtari, A., & Rubin, D. B. (2014). *Bayesian data analysis*. Boca Raton: CRC Press.
- Gilmanov, I., Samigullin, D., Vyskocil, F., Nikolsky, E., & Bukharaeva, E. (2008). Modeling of quantal neurotransmitter release kinetics in the presence of fixed and mobile calcium buffers. *Journal of Computational Neuroscience*, *25*, 296–307.
- Goda, Y., & Stevens, C. F. (1994). Two components of transmitter release at a central synapse. *Proceedings of the National Academy of Sciences*, *91*, 12942–12946.
- Hagler, D. J., & Goda, Y. (2001). Properties of synchronous and asynchronous release during pulse train depression in cultured hippocampal neurons. *Journal of Neurophysiology*, *85*(6), 2324–2334.
- Hefft, S., & Jonas, P. (2005). Asynchronous GABA release generates long-lasting inhibition at a hippocampal interneuron-principal neuron synapse. *Nature Neuroscience*, *8*(10), 1319–1328.
- Kaesler, P. S., & Regehr, W. G. (2014). Molecular mechanisms for synchronous, asynchronous, and spontaneous neurotransmitter release. *Annual Review of Physiology*, *2014*(76), 333–363.
- Katz, B. (1996). Neural transmitter release: from quantal secretion to exocytosis and beyond. The Fenn Lecture. *Journal of Neurocytology*, *25*, 677–686.
- Katz, B., & Miledi, R. (1965). The measurement of synaptic delay and the time course of acetylcholine release at the neuromuscular junction. *Proceedings of the Royal Society B: Biological Sciences*, *161*, 483–495.
- Khuzakhmetova, V., Samigullin, D., Nurullin, L., Vyskocil, F., Nikolsky, E., & Bukharaeva, E. (2014). Kinetics of neurotransmitter release in neuromuscular synapses of newborn and adult rats. *International Journal of Developmental Neuroscience*, *34*, 9–18.
- Lin, J.-W., & Farber, S. (2002). Modulation of synaptic delay during synaptic plasticity. *Trends in Neurosciences*, *25*, 449–455.
- Lu, T., & Trussel, L. O. (2000). Inhibitory transmission mediated by asynchronous transmitter release. *Neuron*, *26*(3), 683–694.
- Matzke, D., Dolan, C. V., Logan, G. D., Brown, S. D., & Wagenmakers, E. J. (2013). Bayesian parametric estimation of stop-signal reaction time distributions. *Journal of Experimental Psychology: General*, *142*(4), 1047–1073. doi:10.3389/fpsyg.2013.00918.
- Minnecci, F., Kanichay, R. T., & Silver, R. A. (2012). Estimation of the time course of neurotransmitter release at central synapses from the first latency of postsynaptic currents. *Journal of Neuroscience Methods*, *205*(1), 49–64. doi:10.1016/j.jneumeth.2011.12.015.
- Muller, D. (1986). Potentiation by 4-aminopyridine of quantal acetylcholine release at the torpedo nerve-electroplaque junction. *Journal of Physiology*, *379*, 479–493.
- Neff, R. A., Conroy, W. G., Schoellerman, J. D., & Berg, D. K. (2009). Synchronous and asynchronous transmitter release at nicotinic synapses are differentially regulated by postsynaptic PSD-95 proteins. *Journal of Neuroscience*, *29*(50), 15770–15779.
- Neher, E., & Sakaba, T. (2008). Multiple roles of calcium ions in the regulation of neurotransmitter release. *Neuron*, *59*, 861–872.
- Nikolsky, E. E., Vyskocil, F., Bukharaeva, E. A., Samigullin, D. V., & Magazanik, L. G. (2004). Cholinergic regulation of the evoked quantal release at frog neuromuscular junction. *Journal of Physiology*, *560*, 77–88.
- Otsu, Y., Shahrezaei, V., Li, B., Raymond, L., Delaney, K., & Murphy, T. (2004). Competition between phasic and asynchronous release for

- recovered synaptic vesicles at developing hippocampal autaptic synapses. *Journal of Neuroscience*, 24, 420–433.
- Pan, B., & Zucker, R. S. (2009). A general model of synaptic transmission and short-term plasticity. *Neuron*, 62(4), 539–554. doi:10.1016/j.neuron.2009.03.025.
- Pang, Z. P., & Sudhof, T. C. (2010). Cell biology of Ca<sup>2+</sup>-triggered exocytosis. *Current Opinion in Cell Biology*, 22, 496–505. doi:10.1016/j.ceb.2010.05.001.
- Parnas, I., & Parnas, H. (2010). Control of neurotransmitter release: from Ca<sup>2+</sup> to voltage dependent G-protein coupled receptors. *Pflugers Archiv / European Journal of Physiology*, 460, 975–990.
- Plummer, M. (2012). Rjags: Bayesian graphical models using MCMC. R package version 3-9. <http://CRAN.R-project.org/package=rjags>.
- Rahamimoff, R., & Yaari, Y. (1973). Delayed release of transmitter at the frog neuromuscular junction. *Journal of Physiology*, 228, 241–257.
- Sabatini, B., & Regehr, W. (1999). Timing of synaptic transmission. *Annual Review of Physiology*, 61, 521–542.
- Smith, S., Chen, W., Vyleta, N., Williams, C., Lee, C.-H., Phillips, C., & Andresen, M. (2012). Calcium regulation of spontaneous and asynchronous neurotransmitter release. *Cell Calcium*, 52, 226–233. doi:10.1016/j.ceca.2012.06.001.
- Stevens, C. F. (1968). Synaptic physiology. *Proceedings of the IEEE*, 56, 916–930.
- Su, Y.-S., & Yajima, M. (2012). R2jags: a package for running jags from R. R package version 0.03–08. <http://CRAN.R-project.org/package=R2jags>.
- Tarr, T. B., Dittrich, M., & Meriney, S. D. (2013). Are unreliable release mechanisms conserved from NMJ to CNS? *Trends in Neuroscience*, 36, 14–22. doi:10.1016/j.tins.2012.09.009.
- Van der Kloot, W. (1988a). Estimating the timing of quantal releases during end-plate currents at the frog neuromuscular junction. *Journal of Physiology*, 402, 595–603.
- Van der Kloot, W. (1988b). The kinetics of quantal releases during end-plate currents at the frog neuromuscular junction. *Journal of Physiology*, 402, 605–626.
- Vyshedskiy, A., & Lin, J. W. (2000). Presynaptic Ca<sup>2+</sup> influx at the inhibitor of the crayfish neuromuscular junction: a photometric study at a high time resolution. *Journal of Neurophysiology*, 83(1), 552–562.
- Wen, H., Hubbard, J. M., Rakela, B., Linhoff, M. W., Mandel, G., & Brehm, P. (2013). Synchronous and asynchronous modes of synaptic transmission utilize different calcium sources. *Elife*, 2, e01206. doi:10.7554/eLife.01206.